Gangliosides are functional nerve cell ligands for myelin-associated glycoprotein (MAG), an inhibitor of nerve regeneration

Alka A. Vyas*, Himatkumar V. Patel*, Susan E. Fromholt*, Marija Heffer-Lauc*, Kavita A. Vyas*, Jiyoung Dang*, Melitta Schachner†, and Ronald L. Schnaar*‡

*Departments of Pharmacology and Neuroscience, The Johns Hopkins School of Medicine, Baltimore, MD 21205; and †Zentrum fuer Molekulare Neurobiologie, Universitaet Hamburg, D-20246 Hamburg, Germany

Communicated by Saul Roseman, The Johns Hopkins University, Baltimore, MD, April 7, 2002 (received for review February 20, 2002)

Myelin-associated glycoprotein (MAG) binds to the nerve cell surface and inhibits nerve regeneration. The nerve cell surface ligand(s) for MAG are not established, although sialic acid-bearing glycans have been implicated. We identify the nerve cell surface gangliosides GD1a and GT1b as specific functional ligands for MAG-mediated inhibition of neurite outgrowth from primary rat cerebellar granule neurons. MAG-mediated neurite outgrowth inhibition is attenuated by (*i*) neuraminidase treatment of the neurons; (*ii*) blocking neuronal ganglioside biosynthesis; (*iii*) genetically modifying the terminal structures of nerve cell surface gangliosides; and (*iv*) adding highly specific IgG-class antiganglioside mAbs. Furthermore, neurite outgrowth inhibition is mimicked by highly multivalent clustering of GD1a or GT1b by using precomplexed antiganglioside Abs. These data implicate the nerve cell surface gangliosides GD1a and GT1b as functional MAG ligands and suggest that the first step in MAG inhibition is multivalent ganglioside clustering.

The adult mammalian central nervous system is an inhibitory environment for nerve regeneration, partially because of specific inhibitors on myelin including myelin-associated glycoprotein (MAG), Nogo, and chondroitin sulfate proteoglycans (1–7). Presumably, these inhibitors bind to specific nerve cell surface ligands, resulting in transmembrane signals that lead to growth cone collapse and inhibition of axon extension. Characterization of nerve cell surface ligands for these inhibitors, and the resulting signal transduction pathways responsible for inhibition, may provide novel approaches to enhance nerve regeneration after injury.

MAG (Siglec-4) is a member of the Siglec family of sialic acid (NeuAc) binding lectins (carbohydrate binding proteins) (8–10). *In vitro* binding studies indicate that MAG binds preferentially to the "NeuAc α3 Gal β3 GalNAc" glycan structure (11), which is prominently expressed on certain gangliosides, sialic acid-bearing glycosphingolipids that comprise major determinants on mammalian nerve cells (12). This observation led to the hypothesis that the major brain gangliosides GD1a and GT1b (Fig. 1) are functional nerve cell surface ligands for MAG (13). Data supporting this hypothesis include that (*i*) MAG binds with high specificity and affinity to GD1a, GT1b, and related gangliosides *in vitro* (14); (*ii*) MAG-ganglioside binding is blocked by a conformationally specific anti-MAG mAb (mAb 513) that also blocks MAG-neuron binding (14); and (*iii*) mice genetically lacking the "NeuAc α3 Gal β3 GalNAc" terminus on gangliosides demonstrate axon degeneration and dysmyelination similar to that in MAG knockout mice (15). These findings led us to propose that gangliosides are functional ligands on nerve cells responsible for MAG-mediated inhibition of nerve regeneration and to probe the molecular mechanism by which inhibition is initiated.

Materials and Methods

Cerebellar Granule Neurons (CGNs). Cell isolation and culture were as described (16). Cerebella were removed from postnatal day 4–5 Sprague–Dawley rats and dissociated enzymatically. CGNs were isolated by the two-step purification method of Hatten (17). Cells at the 35%/60% Percoll interface [>99% neuronal as determined by glial fibrillary acidic protein (GFAP) immunostaining] were collected, washed, and cultured on poly-D-lysine (PDL)-coated microwells at a density of 0.6–1.5 $\times$ 10^5/cm^2 (as indicated). Where indicated, 2.5 μM 1-phenyl-2-hexadecanoylamino-3-morpholino-1-propanol (P4; Matreya, Pleasant Gap, PA) (18), 20 μg/ml of anti-MAG mAb 513 (19), or 7.5 milliunits/ml of neuraminidase (*Vibrio cholerae*, Roche Applied Science or Calbiochem) were included throughout the culture period. P4 is a potent inhibitor of glucosylceramide synthase, the first step in ganglioside biosynthesis. At the concentration used, ganglioside biosynthesis is blocked, and ceramide accumulation is modestly increased (20).

CGNs were also isolated from wild-type mice and mice genetically engineered to lack complex gangliosides [*GalNAcT* (−/−) mice, Fig. 1]. Founder *GalNAcT* mutant mice were kindly

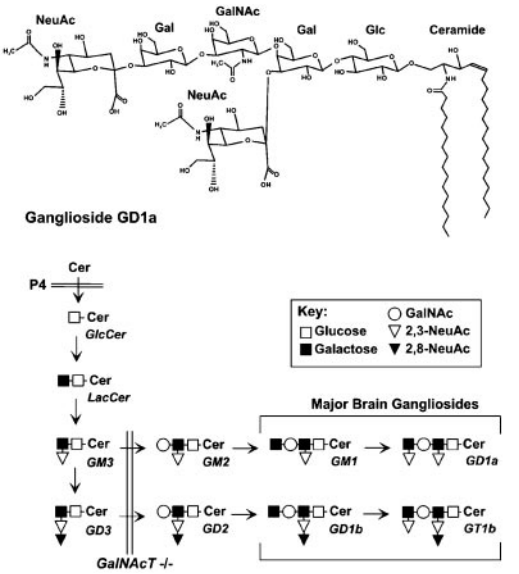

Fig. 1. Ganglioside GD1a and the biosynthetic pathway for major brain gangliosides. [Ganglioside nomenclature is that of Svennerholm (48).] Gangliosides are synthesized by sequential addition of sugars to ceramide by specific glycosyltransferases (49). Pharmacological (P4) and genetic (*GalNAcT* −/−) blocks in the pathway are indicated.

Abbreviations: MAG, myelin-associated glycoprotein; P4, 1-phenyl-2-hexadecanoylamino-3-morpholino-1-propanol; PDL, poly-D-lysine; CGN, cerebellar granule neuron; CHO, Chinese hamster ovary.

See commentary on page 7811.

‡To whom reprint requests should be addressed. E-mail: schnaar@jhu.edu.

www.pnas.org/cgi/doi/10.1073/pnas.072211699

provided by R. Proia, National Institutes of Health, Bethesda (21). Cerebella from postnatal day 4–5 littermates from *GalNAcT* (−/−) female *GalNAcT* (+/−) male breeding pairs were dissected and individually subjected to enzymatic dissociation (16). Dissociated neurons, isolated as described above (16) but without density purification, were plated on test substrata blind to the genotype, which was determined at the end of the experiment by PCR with DNA from tail tissue (15). In some cases, the genotype was confirmed by staining the neurons for complex gangliosides (see below).

Neurite outgrowth was determined after 2 days *in vitro* (see below), at which time newborn rodent CGNs are primarily unipolar, with the neurite often containing a branch morphologically similar to CGN axons developing *in vivo* (22). Cytoskeletal-specific markers have been used to identify early extending neurites from CGNs as axons (22).

Preparation of Inhibitory Substrata. MAG-containing substrata were prepared with two preparations, detergent extract of rat brain myelin (2) and intact membranes from Chinese hamster ovary (CHO) cells expressing MAG (1). For detergent extraction, purified myelin (23) was treated with octyl glucoside (2). Briefly, myelin (1 mg of protein) was suspended in 1 ml of extraction buffer [0.2 M sodium phosphate buffer (pH 6.8) containing 0.1 M Na_2SO_4, 1 mM EDTA, 1 mM DTT, protease inhibitor mixture (Sigma), and 1% octyl glucoside], extracted at 4°C for 16 h, then centrifuged at 400,000 × *g* for 1 h at 4°C. The resulting supernatant was diluted 2-fold with detergent-free extraction buffer and added to PDL-coated tissue culture wells at 75 μg of protein per cm^2 (based on the original myelin protein content). After 4 h at ambient temperature, the plates were washed extensively with PBS and then with culture medium. Cells were plated on control and experimental surfaces and cultured for 48 h, a time point that resulted in reproducible neurite outgrowth on control surfaces.

Alternatively, membranes isolated from CHO cells expressing MAG ["MAG1" or "R2" control CHO transfectants (1)] were adsorbed on culture surfaces. Membranes were prepared from confluent monolayers of MAG1-CHO or R2-CHO cells treated with 100 μM $CdCl_2$ for 16 h before collection. Cells were harvested with a rubber policeman, collected by centrifugation (200 × *g*), washed twice with PBS, and resuspended in homogenization buffer [20 mM Hepes, 1.5 mM $MgCl_2$, 1 mM EGTA, 0.1 M PMSF, and protease inhibitor mixture (Sigma)] for 30 min at 4°C and homogenized in a Dounce homogenizer (45–50 strokes). The suspension was centrifuged at 1,000 × *g* for 10 min at 4°C. The resulting supernatant was centrifuged at 35,000 × *g* for 1 h at 4°C. The membrane pellet was resuspended in 0.32 M sucrose and stored at −70°C. Protein concentration was determined with BCA reagent (Pierce). Only MAG1-CHO membranes bound anti-MAG mAb 513 by ELISA. To prepare membrane-adsorbed substrata, membranes were suspended in PBS at a protein concentration of 0.75 mg/ml, sonicated in a bath sonicator for 30 sec, and then were adsorbed onto PDL-coated tissue culture plates at 112 μg of protein per cm^2 for 4 h. Plates were washed and cells added as described above.

Neurite Outgrowth-Inhibition Assay. After 48 h of culture on control or experimental surfaces, cells were washed with PBS and fixed with 4% paraformaldehyde. In some experiments, cells were plated at a lower density (6×10^4 cells per cm^2) in 24-well plates, and 100–200 cells were scored for neurite outgrowth in each of 5 random microscopic fields. A cell was scored as positive if its neurite length was >4 cell bodies long.

For neurite staining, cells cultured at 1.5×10^5 cells per cm^2 in 96-well plates for 48 h were fixed and permeabilized with methanol at −20°C for 2 min then immunostained with GAP-43 mAb (1:800; Sigma) followed by Cy3-conjugated anti-mouse IgG (1:120; Jackson ImmunoResearch) mixed with 300 nM 4′,6-diamidino-2-phenylindole (Molecular Probes). The cells were washed and random fields from duplicate wells were captured for morphometric analysis (see below) with a Nikon T2000 epifluorescent microscope fitted with a Sony (Tokyo) CCD camera.

Cells plated on control surfaces showed little or no clumping and had long fine neurites that formed a lacy network (e.g., see Fig. 5*A*), whereas on MAG-containing substrata, the cells tended to clump together, as confirmed by 4′,6-diamidino-2-phenylindole staining, and had highly fasciculated neurites (e.g., Fig. 5*B*). Cells on inhibitory substrata extended neurites preferentially on top of existing neurites, whereas on control substrata, single neurites extended onto the substratum independently of one another. This behavior allowed development of an objective semiautomated morphometric method to quantify neurite outgrowth inhibition with METAMORPH (Universal Imaging, Downingtown, PA) image analysis software (see Fig. 7, which is published as supporting information on the PNAS web site, www.pnas.org).

For each experimental condition, images of multiple fields of GAP-43 immunostained cells were acquired from duplicate wells in at least 4 independent experiments. To eliminate pixels stained in the cell body, 4′,6-diamidino-2-phenylindole (DAPI) images were first subtracted from GAP-43 images. The remaining pixels were classified according to their intensity on a 0–255 scale. The intensity of single independent neurites, determined from images of cells on control surfaces, was in the range 51–90. Therefore, the number of pixels with the intensity 51–90 was automatically measured in each image, resulting in a quantitative measure related to the total number of single independent neurites in the image. The image area represented by pixels having the intensity of single neurites was determined and compared between control and experimental cultures and expressed as a percentage. Each data point represents the mean ± SD of neurites quantified from at least 32 images collected from 4 independent experiments. The average number of cells per field in control and experimental wells from any experiment was equivalent (variation ± 2.5% of the mean) as determined by DAPI staining of cell nuclei (data not shown). Statistical *P* values were obtained with a Student's *t* test.

Ganglioside Determinations. Complex gangliosides on fixed neurons were stained by treating with 10 milliunits/ml neuraminidase in DMEM containing 10 mM Hepes and 25 mg/ml of BSA (blocking buffer) for 1 h at 37°C, which converts major complex gangliosides to GM1 (24), a binding ligand for cholera toxin B-subunit (25). The cells were washed and incubated in blocking buffer for 45 min then treated with FITC-labeled cholera toxin B-subunit (5 μg/ml; Sigma) for 1 h.

Antiganglioside mAbs. Highly specific anti-GD1a, anti-GT1b, anti-GD1b, and anti-GM1 IgG1-class mouse mAbs were prepared as described (26, 27). Anti-GD3 (IgG3, R24) was from American Type Culture Collection. Primary Abs (1 mg/ml) were preincubated with or without secondary Ab (0.5 mg/ml; goat anti-mouse IgG Fc-specific, AP conjugate; Jackson ImmunoResearch) in PBS containing 1 mg/ml of BSA for 45 min at 37°C. Rat CGNs were plated on PDL-coated microwells or on substrata coated with detergent-extracted myelin proteins (see above), as indicated. One hour after plating, Abs were added to the growth medium to achieve a final concentration of 10 μg/ml of mAb. After 48 h, cells were fixed, stained with anti-GAP-43 Ab, and single neurites were quantified as described above.

Results

MAG-Mediated Neurite Outgrowth Inhibition Is by Means of a Sialoglycoconjugate. Under our experimental conditions, neurite outgrowth inhibition from CGNs is the result of the interaction

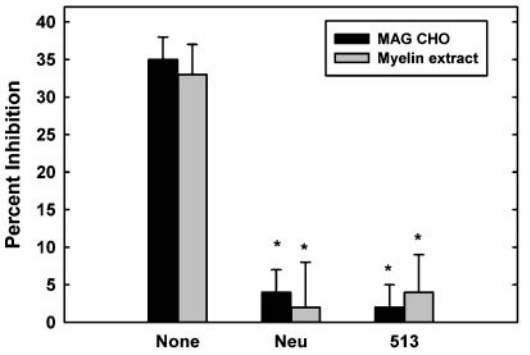

Fig. 2. Neurite outgrowth inhibition by MAG is sialic acid-dependant. CGNs were plated on culture surfaces adsorbed with membranes of MAG-expressing CHO cells or detergent extracts of myelin for 48 h in the presence or absence of neuraminidase (Neu; 7.5 milliunits/ml) or anti-MAG Ab (513; 20 μg/ml). Neurite outgrowth was assessed by scoring the percent of cells with neurites longer than four cell bodies in multiple fields from duplicate wells per experiment. Data are normalized with respect to the appropriate control (membranes of control CHO cells or detergent-containing buffer, respectively). Data are presented as the mean $\pm$ SD of at least 3 independent experiments. *, $P < 0.005$.

between nerve cell surface sialoglycoconjugates and substrate-adsorbed MAG (Fig. 2). Two experimental systems were used. In one, CGNs were plated on substrata adsorbed with a detergent extract of myelin, which includes MAG (2). In the other, substrata were adsorbed with sonicated membranes from MAG-expressing CHO cells (1). Both substrata caused reproducible inhibition of neurite outgrowth, which was quantified by scoring the number of cells with neurites longer than 4 cell bodies in at least 5 random fields (cells in large clumps were not included in the analyses). A monoclonal anti-MAG Ab that specifically blocks MAG-nerve cell binding (mAb 513) completely reversed the inhibitory activity of both substrata (Fig. 2), whereas isotype-matched IgG (anti-Thy-1) did not result in any reversal of inhibition (data not shown). Furthermore, treatment with *V. cholerae* neuraminidase, which cleaves most cell surface sialic acids, reversed the inhibition of neurite outgrowth on both types of inhibitory substrata (Fig. 2) but did not affect neurite outgrowth on control substrata, consistent with a prior report (28). Taken together these results show that the inhibition of neurite outgrowth under our conditions is MAG-mediated and sialic acid-dependent. Of interest, *V. cholerae* neuraminidase treatment is effective only on the outermost sialic acids of gangliosides (24), converting the MAG-binding gangliosides GD1a and GT1b to the nonbinding ganglioside GM1, without altering the total membrane concentration of complex gangliosides.

Blocking Ganglioside Biosynthesis Reverses MAG-Mediated Neurite Outgrowth Inhibition. MAG preferentially binds to sialylated glycans containing the structure "NeuAc α3 Gal β3 GalNAc" (11), a determinant found chiefly on neuronal cell surface gangliosides (12). MAG binds with high specificity and affinity to the major brain gangliosides GD1a and GT1b that carry this determinant (14). These gangliosides are abundant on nerve cell surfaces, including CGNs (29) and their nascent axonal processes (27). Therefore, we probed whether gangliosides are functional ligands for MAG-mediated inhibition of nerve regeneration by using a glucosylceramide synthase inhibitor, P4 (18), which blocks synthesis of all glycosphingolipids, including gangliosides. Importantly, glucosylceramide synthase inhibitors do not directly affect glycoprotein biosynthesis, and P4 does not reduce cell viability or neurite outgrowth (30, 31). Because of the relatively rapid turnover of gangliosides on the surface of CGNs in culture ($t_{1/2} < 12$ h, data not shown), P4 efficiently depleted

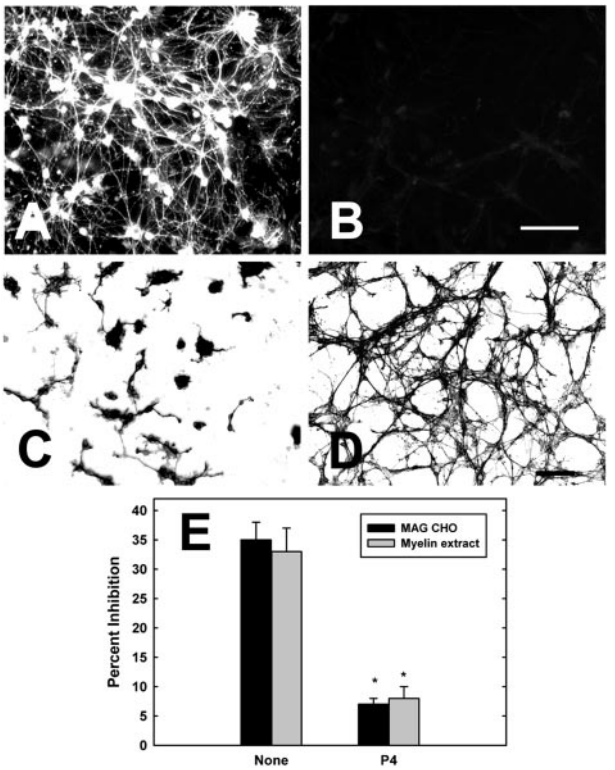

Fig. 3. Blocking glycosphingolipid biosynthesis reverses MAG-mediated inhibition of neurite outgrowth. Rat CGNs were treated without (control, *A*) or with (*B*) the glycosphingolipid biosynthetic inhibitor P4 (2.5 μM) for 48 h. Cell surface complex gangliosides were detected by neuraminidase treatment followed by labeling with FITC-cholera toxin B-subunit as described in *Materials and Methods*. Fluorescent images of the cholera B-subunit-labeled cultures (*A* and *B*) demonstrate nearly complete depletion of complex cell surface gangliosides after P4 treatment. In separate experiments, cells were cultured on MAG-containing inhibitory substrata in the absence (control, *C*) or presence of 2.5 μM P4 (*D*). After 48 h, cells were immunostained for GAP-43 and visualized by Cy3-conjugated secondary Ab to detect neurites [images are presented as the reverse grayscale (black on white) for clarity], revealing enhanced neurite outgrowth by P4-treated neurons. Neurite outgrowth inhibition, quantified as described in the legend to Fig. 2, is presented as the mean $\pm$ SD of at least 3 independent experiments (*E*). *, $P < 0.005$. (Bars = 50 μm.) Equivalent reversal of neurite outgrowth inhibition by P4 treatment was quantified with semiautomated image analysis (see Fig. 7).

cell surface gangliosides. After 48 h in the presence of 2.5 μM, P4 cell surface gangliosides were nearly undetectable, whereas control cells expressed abundant complex gangliosides (Fig. 3 *A* and *B*). Ganglioside depletion was confirmed with thin-layer chromatography of whole cell extracts (data not shown). Cells depleted of gangliosides were significantly less responsive to MAG-mediated neurite outgrowth inhibition in either of the two experimental systems used (Fig. 3 *C* and *D*). Whether quantified microscopically as the percent of neurons with neurites (Fig. 3*E*) or with semiautomated image analysis (see Fig. 7), nearly identical reversal of MAG-mediated inhibition was independently confirmed. These results suggest that glycosphingolipids are major neuronal targets for MAG. To test whether gangliosides bearing the "NeuAc α3 Gal β3 GalNAc" terminus were functional MAG targets, nerve cells from genetically engineered mice were used.

Nerve Cells from Mice Engineered to Lack Complex Gangliosides Are Less Susceptible to MAG-Mediated Inhibition. Complex gangliosides are synthesized from simpler precursors by the addition of GalNAc to the growing carbohydrate chain via the enzyme

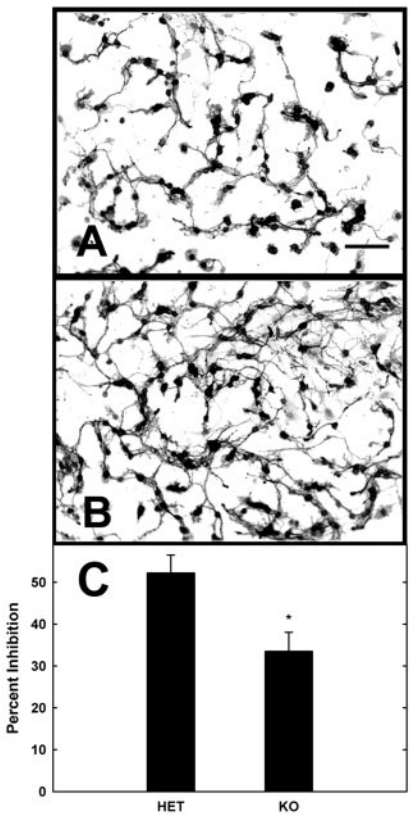

Fig. 4. Neurons from complex ganglioside knockout mice are less responsive to MAG-mediated neurite outgrowth inhibition. CGNs from *GalNAcT* heterozygote (*A*) and knockout mice (*B*) were grown for 48 h on substrata adsorbed with a detergent extract of myelin and then were immunostained for GAP-43. Images are presented as the reverse grayscale (black on white) for clarity. (Bar = 50 μm.) Neurite outgrowth inhibition from 25 heterozygote and 21 knockout littermates, quantified by image analysis as described in *Materials and Methods* (presented as mean ± SD), indicates that neurons lacking complex gangliosides are significantly less susceptible to MAG-mediated neurite outgrowth inhibition (*C*). *, $P < 0.01$.

UDP-*N*-acetylgalactosamine:GM3/GD3 *N*-acetylgalactosaminyltransferase (GalNAcT). Knockout mice with an inactivated *GalNAcT* gene (21) do not express complex gangliosides such as GD1a and GT1b (Fig. 1). Instead, these mice express compensatory amounts of the simpler gangliosides GD3 (which is not a MAG ligand) and GM3 (which binds MAG, but with lower affinity than GD1a or GT1b) (14, 21). Heterozygotes express the same series of complex gangliosides as wild-type mice. To test the role of complex ganglioside termini in MAG-mediated neurite outgrowth inhibition, we plated neurons from *GalNAcT* knockout and heterozygote littermates, blind to the genotype, on PDL- and MAG-coated substrata. The genotype was determined at the end of the experiment by PCR, and ganglioside expression was confirmed by immunostaining (data not shown). Neurons from *GalNAcT* +/− mice, which express complex gangliosides, were fully susceptible to MAG inhibition (Fig. 4*A*). In contrast, neurons from *GalNAcT* −/− littermates lacked complex gangliosides and showed reduced inhibition compared with matched controls (Fig. 4 *B* and *C*). Cells from either genotype extended identical, well defined neurites on control surfaces (data not shown).

Although *GalNAcT* −/− neurons were less sensitive to MAG-mediated neurite outgrowth inhibition than control neurons, the magnitude of the difference was less than that found with P4- or neuraminidase-treated neurons (compare Fig. 4*C* to Figs. 2 and 3*E*). Whereas treatment with P4 or neuraminidase eliminates all MAG-binding ganglioside determinants, *GalNAcT* −/− neurons express a relatively high amount of GM3, which binds MAG, albeit with less avidity than GD1a or GT1b (14). Therefore, *GalNAcT* −/− neurons may retain an attenuated response by means of MAG binding to GM3.

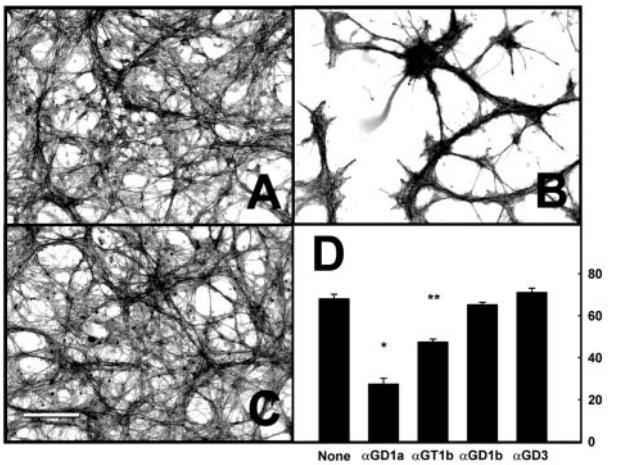

Fig. 5. IgG-class mouse mAbs against GD1a or GT1b attenuate MAG-mediated neurite outgrowth inhibition. CGNs were grown on PDL- (*A*) or MAG-adsorbed surfaces (*B* and *C*) in the absence (*B*) or presence (*C*) of 10 μg/ml of anti-GD1a monoclonal IgG. Images are presented as the reverse grayscale (black on white) for clarity. (Bar = 100 μm.) The effects of adding 10 μg/ml of the indicated antiganglioside Abs on MAG-mediated neurite outgrowth inhibition were quantified by image analysis (*D*), as described in *Materials and Methods*, and are presented as mean percent inhibition ± SD. *, $P < 0.002$; **, $P < 0.02$.

Abs Against GD1a and GT1b Block MAG-Mediated Inhibition of Neurite Outgrowth. Monoclonal antiganglioside Abs were added to cultures of neuronal cells 1 h after plating on control and inhibitory substrata. After 48 h, the cells were fixed and neurite outgrowth was quantified. Anti-GD1a Ab sharply reduced MAG-mediated inhibition, anti-GT1b Ab had an intermediate effect, whereas anti-GD1b or anti-GD3 Abs had no effect (Fig. 5).

Multivalent Clustering of GD1a or GT1b Inhibits Neurite Outgrowth. One mechanism by which MAG may initiate inhibition of neurite outgrowth is by multivalent clustering of target gangliosides on the nerve cell surface. Data supporting this hypothesis was reported by Vinson *et al.* (32) by using a decavalent anti-GT1b mouse monoclonal IgM. Bivalent IgG-class antiganglioside Abs did not inhibit neurite outgrowth on control substrata (Figs. 6 *A* and *C*) and instead blocked MAG-mediated inhibition (Fig. 5). To resolve this apparent discrepancy, we determined whether higher-order multivalent clustering of gangliosides might inhibit neurite outgrowth. When the IgG-class anti-GD1a or anti-GT1b Abs were precomplexed with a goat anti-mouse polyclonal Ab, marked inhibition was seen (Fig. 6*D*). The morphological changes induced were similar to those induced by MAG (either as myelin extract or as MAG-CHO cell membranes) in that cell bodies were clustered and neurites were fasciculated. Automated morphometry revealed >50% inhibition of neurite outgrowth by precomplexed anti-GD1a and anti-GT1b Abs (Fig. 6*E*). In contrast, precomplexed anti-GM1 IgG was without effect (Fig. 6 *B* and *E*). These data indicate that multivalent Ab-induced clustering of the MAG target gangliosides GD1a or GT1b mimics MAG-mediated neurite outgrowth.

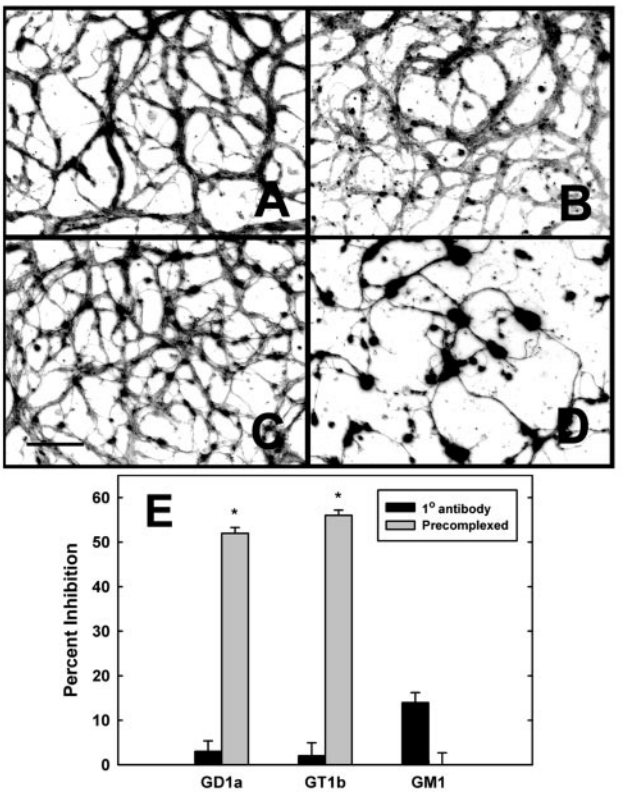

Fig. 6. Clustering complex gangliosides on neuronal surfaces inhibits neurite outgrowth. CGNs grown on PDL-coated surfaces were treated for 48 h with 10 μg/ml of anti-GM1 mAb (*A* and *B*) or anti-GD1a mAb (*C* and *D*). Abs were added either alone (*A* and *C*) or after precomplexing for 1 h with anti-mouse IgG (5 μg/ml; *B* and *D*). Neurites were visualized by GAP-43 immunostaining, with images presented as the reverse grayscale (black on white) for clarity. (Bar = 100 μm.) Neurite outgrowth inhibition was quantified by image analysis (*E*) as described in *Materials and Methods*. *, $P < 0.0002$ (the small inhibitory effect of uncomplexed anti-GM1 mAb was not statistically significant, $P > 0.15$).

Discussion

The lack of recovery after central nervous system (e.g., spinal cord) injury is caused, in part, by myelin inhibitors including MAG, Nogo, and a chondroitin sulfate proteoglycan (1–7, 33). A functional Nogo ligand on nerve cells, a glycosylphosphatidylinositol (GPI)-anchored membrane glycoprotein, was recently discovered (5). In contrast, functional nerve cell surface ligand(s) for MAG have not been established. The data reported here demonstrate that the gangliosides GD1a and GT1b serve as functional MAG ligands.

The discovery that MAG is a member of the Siglec family of sialic acid-binding proteins has led to the hypothesis that nerve cell surface sialoglycoconjugates are functional MAG ligands (8). Initial specificity studies implicated a particular extended glycan structure "NeuAc α3 Gal β3 GalNAc" as the preferred MAG target (11). This terminal structure is found on some O-linked glycoproteins throughout the body, but in the mammalian brain it is much more abundant on gangliosides GD1a and GT1b (12). Direct binding studies confirmed potent and highly specific MAG binding to these gangliosides (14, 34). Furthermore, mice engineered to lack the "NeuAc α3 Gal β3 GalNAc" terminus on gangliosides (but not on glycoproteins) displayed axon degeneration and dysmyelination similar to mice lacking MAG (15). These data were consistent with a role for gangliosides as MAG ligands in myelin stabilization, but did not address the potential of gangliosides to serve as MAG ligands in the inhibition of nerve regeneration.

Published reports seemed to conflict regarding the role of sialoglycoconjugates as MAG ligands. DeBellard *et al.* (28) reported that neuraminidase treatment attenuated the neurite inhibitory effects of MAG on CGNs and dorsal root ganglion neurons, supporting a role for sialoglycoconjugates. Subsequently, Tang *et al.* (35) reported that a soluble chimeric form of MAG (MAG-Fc) with a mutated Arg-118, a key sialic acid-binding residue, failed to bind neurons and failed to inhibit neurite outgrowth, further implicating sialic acid binding in neurite inhibition. Paradoxically, when full-length MAG bearing the R118 mutation was expressed on the surface of CHO cells, it inhibited neurite outgrowth. Although the authors concluded that "the sialic acid binding of MAG may promote, but may not be essential for" (35) the inhibitory effect of MAG, subsequent work from Vinson *et al.* (32) challenged this conclusion. They found that the residual inhibition by the R118 mutant was also sialic acid-dependent. These data indicate that the R118-mutant MAG retains sufficient sialic acid binding to inhibit neurite outgrowth when the protein is expressed in a highly multivalent form on the surface of CHO cells (36).

The data reported here are consistent with the hypothesis that nerve cell surface gangliosides are both necessary and sufficient to support MAG-mediated neurite outgrowth inhibition from CGNs. Gangliosides are necessary in that blocking their biosynthesis pharmacologically or genetically attenuates MAG inhibition (Figs. 3 and 4). They are sufficient in that specific crosslinking of cell surface gangliosides GD1a or GT1b mimics the inhibitory effect of MAG (Fig. 6).

Although our data implicate gangliosides as functional MAG ligands, they do not exclude other potential ligands. Some published data identify sialoglycoproteins as MAG binding ligands, but evidence for their function remains inconclusive. Extensive trypsin treatment of CGNs partially inhibited binding of a MAG-Fc chimera (28). Although the authors interpret this result as implicating a sialoglycoprotein, the data are equally consistent with gangliosides being the functional MAG-binding sialoglycoconjugates, because over half of the binding was protease-resistant. The study did not address whether the protease-sensitive or -resistant binding sites (or both) were functional. Published studies reporting the identification of particular MAG-binding sialoglycoproteins also did not address their function (37, 38). MAG and MAG chimeras bind both to functional and nonfunctional sialoglycoconjugates [e.g., human erythrocytes (8)]. An experimental challenge is to distinguish which sialoglycoconjugates function to inhibit nerve regeneration. Our data indicate that gangliosides GD1a and GT1b, the most abundant MAG-binding glycoconjugates in the brain, are necessary and sufficient nerve cell surface ligands for MAG in our experimental system. Other MAG-binding sialoglycoconjugates may also be functional but have yet to be fully evaluated.

Vinson *et al.* (32), using hippocampal neurons, reported that IgM-induced clustering of GT1b, but not GD1a, inhibited neurite outgrowth, whereas we found that anti-GD1a and anti-GT1b, when appropriately crosslinked, were equally effective. Because GD1a and GT1b are major gangliosides on both CGNs (29) and hippocampal neurons (39), the distinction may reflect differences in affinities of the mAbs used or differences in downstream signaling in the different nerve cell types.

The data in Fig. 6 imply that the initial mechanism leading to neurite outgrowth inhibition is ganglioside clustering. Bivalent IgG antiganglioside mAbs were ineffective unless they were crosslinked further with secondary Ab. The ability of uncrosslinked anti-GD1a mAb to block MAG inhibition (Fig. 5) implicates ganglioside clustering as a primary event in MAG-mediated inhibition of nerve regeneration. Although MAG is a quantitatively minor component of central nervous system my-

elin (~1% of myelin protein), in the adult it is concentrated on periaxonal membranes (40) where it may be densely spaced and provide for effective multivalent clustering of gangliosides.

The mechanism(s) by which ganglioside clustering results in subsequent signaling within the neuron remain a focus for future study. Initial pharmacological manipulation implicates a role for the Rho GTPase (32), which partitions (along with gangliosides) into membrane rafts (41) that have also been termed "glycosignaling domains" (42), based on the signaling molecules enriched there. It may be significant that GD1a is enriched in these domains (relative to other gangliosides) in CGNs in culture (29). In separate studies, Ab-induced crosslinking of ganglioside GM3 in melanoma cells (43) or GD3 in neurons (44) resulted in activation of raft-resident signaling molecules (Src and Lyn, respectively). These data established a potential functional link between ganglioside crosslinking and intracellular signaling pathways. We hypothesize that multivalent crosslinking of GD1a or GT1b by MAG may lead, directly or via transmembrane adapter molecules, to alterations in raft-resident signaling molecules that may include Rho, Src family members, or others.

The complete signaling system is likely to be complex. MAG acts as a neurite outgrowth inhibitor for most neurons tested but stimulates neurite outgrowth in immature dorsal root ganglion neurons (28). Thus, the effect of MAG on neurons may depend on the intracellular context in which the signal is generated, as evidenced by alterations in the actions of MAG by modulators of intracellular cyclic nucleotide-signaling pathways (45, 46). It is noteworthy that the ligand for Nogo, a glycosylphosphatidylinositol-anchored protein (5), is, like ganglioside, likely to partition into membrane rafts and may use a raft-related mechanism for transmembrane signaling (47). Identification of nerve cell surface gangliosides as functional MAG ligands provides new directions and tools to unravel these inhibitory signaling mechanisms.

We thank Dr. Richard L. Proia for providing founders for the GalNAcT mutant mouse colony. This work was supported by grants from the National Institutes of Health (NS37096), the National Multiple Sclerosis Society (RG2820), and the Stollof Family Fund.

1. Mukhopadhyay, G., Doherty, P., Walsh, F. S., Crocker, P. R. & Filbin, M. T. (1994) *Neuron* **13,** 757–767.
2. McKerracher, L., David, S., Jackson, D. L., Kottis, V., Dunn, R. J. & Braun, P. E. (1994) *Neuron* **13,** 805–811.
3. Chen, M. S., Huber, A. B., van der Haar, M. E., Frank, M., Schnell, L., Spillmann, A. A., Christ, F. & Schwab, M. E. (2000) *Nature (London)* **403,** 434–439.
4. Fidler, P. S., Schuette, K., Asher, R. A., Dobbertin, A., Thornton, S. R., Calle-Patino, Y., Muir, E., Levine, J. M., Geller, H. M., Rogers, J. H., *et al.* (1999) *J. Neurosci.* **19,** 8778–8788.
5. Fournier, A. E., GrandPre, T. & Strittmatter, S. M. (2001) *Nature (London)* **409,** 341–346.
6. GrandPre, T., Nakamura, F., Vartanian, T. & Strittmatter, S. M. (2000) *Nature (London)* **403,** 439–444.
7. Prinjha, R., Moore, S. E., Vinson, M., Blake, S., Morrow, R., Christie, G., Michalovich, D., Simmons, D. L. & Walsh, F. S. (2000) *Nature (London)* **403,** 383–384.
8. Kelm, S., Pelz, A., Schauer, R., Filbin, M. T., Song, T., de Bellard, M. E., Schnaar, R. L., Mahoney, J. A., Hartnell, A., Bradfield, P., *et al.* (1994) *Curr. Biol.* **4,** 965–972.
9. Crocker, P. R. & Varki, A. (2001) *Immunology* **103,** 137–145.
10. Schachner, M. & Bartsch, U. (2000) *Glia* **29,** 154–165.
11. Crocker, P. R., Kelm, S., Hartnell, A., Freeman, S., Nath, D., Vinson, M. & Mucklow, S. (1996) *Biochem. Soc. Trans.* **24,** 150–156.
12. Schnaar, R. L. (2000) in *Carbohydrates in Chemistry and Biology, Part II: Biology of Saccharides*, eds. Ernst, B., Hart, G. W. & Sinaÿ, P. (Wiley–VCH, Weinheim, Germany), pp. 1013–1027.
13. Vyas, A. A. & Schnaar, R. L. (2001) *Biochimie* **83,** 677–682.
14. Collins, B. E., Kiso, M., Hasegawa, A., Tropak, M. B., Roder, J. C., Crocker, P. R. & Schnaar, R. L. (1997) *J. Biol. Chem.* **272,** 16889–16895.
15. Sheikh, K. A., Sun, J., Liu, Y., Kawai, H., Crawford, T. O., Proia, R. L., Griffin, J. W. & Schnaar, R. L. (1999) *Proc. Natl. Acad. Sci. USA* **96,** 7532–7537.
16. Vyas, K. A., Patel, H. V., Vyas, A. A. & Schnaar, R. L. (2001) *Biol. Chem.* **382,** 241–250.
17. Hatten, M. E. (1985) *J. Cell Biol.* **100,** 384–396.
18. Abe, A., Radin, N. S., Shayman, J. A., Wotring, L. L., Zipkin, R. E., Sivakumar, R., Ruggieri, J. M., Carson, K. G. & Ganem, B. (1995) *J. Lipid Res.* **36,** 611–621.
19. Poltorak, M., Sadoul, R., Keilhauer, G., Landa, C., Fahrig, T. & Schachner, M. (1987) *J. Cell Biol.* **105,** 1893–1899.
20. Rani, C. S., Abe, A., Chang, Y., Rosenzweig, N., Saltiel, A. R., Radin, N. S. & Shayman, J. A. (1995) *J. Biol. Chem.* **270,** 2859–2867.
21. Liu, Y., Wada, R., Kawai, H., Sango, K., Deng, C., Tai, T., McDonald, M. P., Araujo, K., Crawley, J. N., Bierfreund, U., *et al.* (1999) *J. Clin. Invest.* **103,** 497–505.
22. Powell, S. K., Rivas, R. J., Rodriguez-Boulan, E. & Hatten, M. E. (1997) *J. Neurobiol.* **32,** 223–236.
23. Norton, W. T. & Poduslo, S. E. (1973) *J. Neurochem.* **21,** 749–757.
24. Schauer, R., Rudiger, W. V., Sander, M., Corfield, A. P. & Wiegandt, H. (1980) *Adv. Exp. Med. Biol.* **125,** 283–294.
25. Holmgren, J., Lonnroth, I. & Svennerholm, L. (1973) *Infect. Immun.* **8,** 208–214.
26. Lunn, M. P., Johnson, L. A., Fromholt, S. E., Itonori, S., Huang, J., Vyas, A. A., Hildreth, J. E., Griffin, J. W., Schnaar, R. L. & Sheikh, K. A. (2000) *J. Neurochem.* **75,** 404–412.
27. Schnaar, R. L., Fromholt, S. E., Gong, Y., Vyas, A. A., Laroy, W., Wayman, D. M., Heffer-Lauc, M., Ito, H., Ishida, H., Kiso, M., *et al.* (2002) *Anal. Biochem.* **302,** 276–284.
28. DeBellard, M.-E., Tang, S., Mukhopadhyay, G., Shen, Y.-J. & Filbin, M. T. (1996) *Mol. Cell. Neurosci.* **7,** 89–101.
29. Prinetti, A., Chigorno, V., Prioni, S., Loberto, N., Marano, N., Tettamanti, G. & Sonnino, S. (2001) *J. Biol. Chem.* **276,** 21136–21145.
30. Paul, P., Bordmann, A., Rosenfelder, G. & Towbin, H. (1992) *Anal. Biochem.* **204,** 265–272.
31. Li, R., Kong, Y. & Ladisch, S. (1998) *Glycobiology* **8,** 597–603.
32. Vinson, M., Strijbos, P. J., Rowles, A., Facci, L., Moore, S. E., Simmons, D. L. & Walsh, F. S. (2001) *J. Biol. Chem.* **276,** 20280–20285.
33. GrandPre, T. & Strittmatter, S. M. (2001) *Neuroscientist* **7,** 377–386.
34. Yang, L. J. S., Zeller, C. B., Shaper, N. L., Kiso, M., Hasegawa, A., Shapiro, R. E. & Schnaar, R. L. (1996) *Proc. Natl. Acad. Sci. USA* **93,** 814–818.
35. Tang, S., Shen, Y. J., de Bellard, M. E., Mukhopadhyay, G., Salzer, J. L., Crocker, P. R. & Filbin, M. T. (1997) *J. Cell Biol.* **138,** 1355–1366.
36. Lee, R. T. & Lee, Y. C. (2000) *Glycoconj. J.* **17,** 543–551.
37. de Bellard, M. E. & Filbin, M. T. (1999) *J. Neurosci. Res.* **56,** 213–218.
38. Strenge, K., Schauer, R. & Kelm, S. (1999) *FEBS Lett.* **444,** 59–64.
39. Hirschberg, K., Zisling, R., Echten-Deckert, G. & Futerman, A. H. (1996) *J. Biol. Chem.* **271,** 14876–14882.
40. Trapp, B. D., Andrews, S. B., Cootauco, C. & Quarles, R. (1989) *J. Cell Biol.* **109,** 2417–2426.
41. Simons, K. & Toomre, D. (2000) *Nat. Rev. Mol. Cell Biol.* **1,** 31–39.
42. Hakomori, S. (2002) *Proc. Natl. Acad. Sci. USA* **99,** 225–232.
43. Iwabuchi, K., Yamamura, S., Prinetti, A., Handa, K. & Hakomori, S. (1998) *J. Biol. Chem.* **273,** 9130–9138.
44. Kasahara, K., Watanabe, Y., Yamamoto, T. & Sanai, Y. (1997) *J. Biol. Chem.* **272,** 29947–29953.
45. Song, H., Ming, G., He, Z., Lehmann, M., Tessier-Lavigne, M. & Poo, M. (1998) *Science* **281,** 1515–1518.
46. Cai, D., Shen, Y., De Bellard, M., Tang, S. & Filbin, M. T. (1999) *Neuron* **22,** 89–101.
47. Brown, D. A. & London, E. (1998) *Annu. Rev. Cell Dev. Biol.* **14,** 111–136.
48. Svennerholm, L. (1994) *Prog. Brain Res.* **101,** xi–xiv.
49. van Echten, G. & Sandhoff, K. (1993) *J. Biol. Chem.* **268,** 5341–5344.